



## **Hybrid MPPT Technique Using Fuzzy Logic and Ant Colony for Effective Solar Pumping Head**

**P.Marish Kumar\*, R.Keerthana, K.A.Indu Sailaja,  
Sathiya.J , Tamil Arasi.T, Swarna Priya Dharshini.J, Sabarinathan.P**

**Easwari Engineering College, Electrical and Electronics Engineering Faculty &  
Student, Chennai, India**

**Abstract :** Solar cells convert energy from sun directly into electricity. Solar photovoltaic modules are where the electricity gets generated, but are only one of the many parts in a complete photovoltaic (PV) system. For the generated electricity to be useful in a home or business, several other technologies must be in place. The non-linear nature of IV curve of the PV system makes it necessary to use some technique to track the maximum voltage and maximum current point on IV curve corresponding to Maximum Power Point(MPP). Thus, Maximum Power Point Tracking (MPPT) techniques are widely used for this purpose. Currently there are many MPPT algorithms in use but they have some problems. For example, perturb and observe (P & O) method will cause oscillations around the maximum power point. It is perceived that the use of two MPPT algorithms in pair will help to overcome the drawbacks of individual MPPT algorithms used in isolation. This paper proposes two MPPT algorithms, such as Fuzzy logic and Ant colony technique to overcome the inherited deficiencies found in *P&O* technique. Even under the frequent changing irradiance conditions, the proposed MPPT technique is much more robust in tracking the MPP and is less oscillatory around the MPP as compared to *P&O*.

**Keywords :** Photovoltaic(PV) cell, Maximum Power Point Tracking (MPPT), Perturb and observe (P&O) Fuzzy Logic, Ant Colony, Hybrid Algorithm.

### **I. Introduction**

Even though many energy sources are available in the world, one of the most important renewable energy sources is solar energy. It is easily available compared to other energy sources and supply large amount of energy to the earth. Solar energy is clean and free of emissions, since it does not produce any pollution or harmful to the nature. The power generated by the PV systems can be either directly supplied to the buildings or fed back into the electrical grid to reduce the high economic costs and environmental impact, associated with the traditional energy sources such as nuclear power and fossil fuels. Nowadays the conversion of solar energy into electrical energy has become very popular and creates many research areas. Solar water pumping system is a modern methodology but it is not a field proven means of pumping water in locations where access to grid power is not available, or where the grid is not reliable. These systems use photovoltaic (PV) cells to convert sunlight into electricity to power DC pumps which can be used to pump groundwater or surface water. This system provides the power at all time even at cloudy days. To increase the efficiency of irrigation in agriculture, this system can be used supply DC power which can be used for pumping application. DC-DC boost converter used in pumping system is to stabilize the voltage for permanent magnet DC motor. The boost converter is used to step up the input voltage. A solar photovoltaic water pumping system (SPWPS) consists of PV array, motor-

pump set, associated electronics and an ON/OFF switch. PV systems usually suffer from low energy conversion efficiency, and it is therefore necessary to improve their performance by tackling the energy loss issues. The maximum power point tracking (MPPT) control technique is essential to the PV assisted generation systems to achieve the maximum power output in real time.

## ii. Modeling of Solar Array

### 1. Theory of I-V Characterization

PV cells can be modelled as a current source in parallel with a diode. When there is no light present to generate any current, the PV cell behaves like a diode. As the intensity of incident light increases, current is generated by the PV cell, as illustrated in Figure 1.

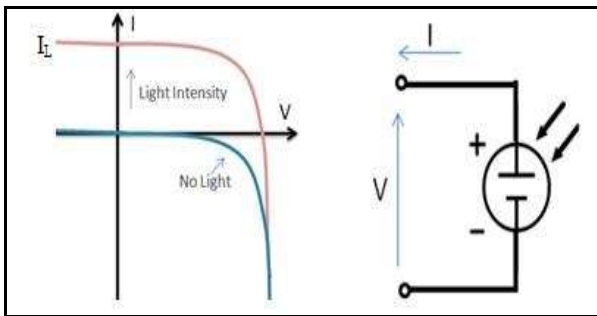


**Figure 1: I-V Curve of PV Cell and Associated Electrical Diagram**

In an ideal cell, the total current  $I$  is equal to the current  $I_L$  generated by the photoelectric effect minus the diode current  $I_D$ , according to the equation:

$$I = I_L - I_D = I_L - I_0 \left( e^{\frac{qV}{kT}} - 1 \right)$$

where  $I_0$  is the saturation current of the diode,  $q$  is the elementary charge  $1.6 \times 10^{-19}$  Coulombs,  $k$  is a constant of value  $1.38 \times 10^{-23}$  J/K,  $T$  is the cell temperature in Kelvin, and  $V$  is the measured cell voltage that is either produced (power quadrant) or applied (voltage bias). A more accurate model will include two diode terms; however, single diode model is approximated in this paper.

Expanding the equation gives the simplified circuit model shown below and the following associated equation, where  $n$  is the diode idealist factor (typically between 1 and 2), and  $R_S$  and  $R_{SH}$  represents the series and shunt resistances that are described in further detail later in this document:

$$I = I_L - I_0 \left( \exp \frac{q(V+I \cdot R_S)}{n \cdot k \cdot T} - 1 \right) - \frac{V + I \cdot R_S}{R_{SH}}$$

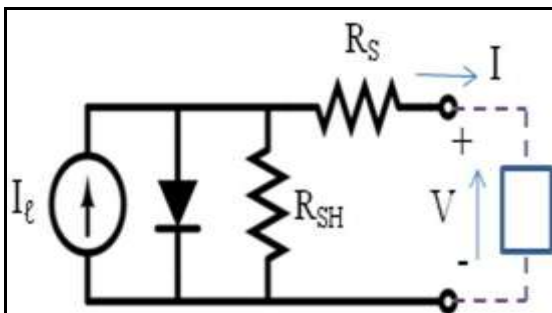


**Figure 2: Simplified Equivalent Circuit Model for a Photovoltaic Cell**

The I-V curve of an illuminated PV cell has the shape shown in Figure 3 as the voltage across the measuring load is swept from zero to  $V_{OC}$ , and many performance parameters for the cell can be determined from this data, as described in the sections below.

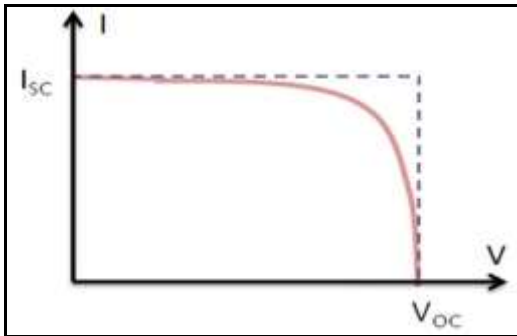


Figure 3: Illuminated I-V Sweep Curve

### Short Circuit Current ( $I_{SC}$ )

The short circuit current  $I_{SC}$  corresponds to the short circuit condition when the impedance is low and is calculated when the voltage equals 0.  $I$  (at  $V=0$ ) =  $I_{SC}$

$I_{SC}$  occurs at the beginning of the forward-bias sweep and is the maximum current value in the power quadrant. For an ideal cell, this maximum current value is the total current produced in the solar cell by photon excitation.

$$I_{SC} = I_{MAX} = I_t \text{ for forward-bias power quadrant}$$

### Open Circuit Voltage ( $V_{OC}$ )

The open circuit voltage ( $V_{OC}$ ) occurs when there is no current passing through the cell.

$$V \text{ (at } I=0) = V_{OC}$$

$V_{OC}$  is also the maximum voltage difference across the cell for a forward-bias sweep in the power quadrant.  $V_{OC} = V_{MAX}$  for forward-bias power quadrant

### Maximum Power ( $P_{MAX}$ ), Current at $P_{MAX}$ ( $I_{MP}$ ), Voltage at $P_{MAX}$ ( $V_{MP}$ )

The power produced by the cell in Watts can be easily calculated along the I-V sweep by the equation  $P=IV$ . At the  $I_{SC}$  and  $V_{OC}$  points, the power will be zero and the maximum value for power will occur between the two. The voltage and current at this maximum power point are denoted as  $V_{MP}$  and  $I_{MP}$  respectively.

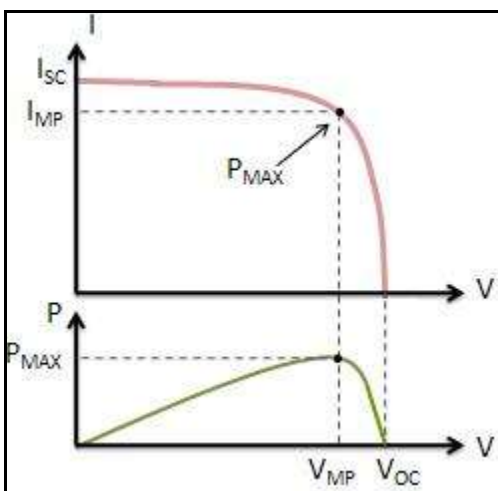
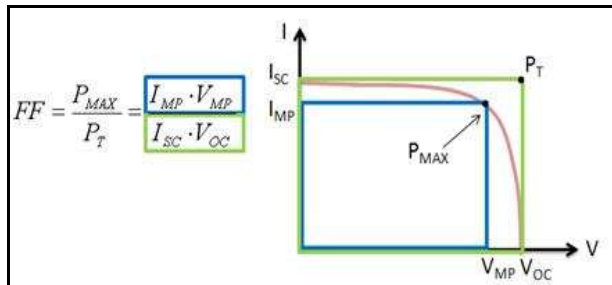


Figure 4: Maximum Power for an I-V Sweep

**Fill Factor (FF)**

The Fill Factor (FF) is essentially a measure of quality of the solar cell. It is calculated by comparing the maximum power to the theoretical power ( $P_T$ ) that would be output at both the open circuit voltage and short circuit current together. FF can also be interpreted graphically as the ratio of the rectangular areas depicted in Figure 5. A larger fill factor is desirable, and corresponds to an I-V sweep that is more square-like. Typical fill factors range from 0.5 to 0.82. Fill factor is also often represented as a percentage.



**Figure 5: Getting the Fill Factor from the I-V Sweep**

**Efficiency ( $\eta$ )**

Efficiency is the ratio of the electrical power output  $P_{out}$ , compared to the solar power input,  $P_{in}$ , into the PV cell.  $P_{out}$  can be taken to be  $P_{MAX}$  since the solar cell can be operated up to its maximum power output to get the maximum efficiency.

$$\eta = \frac{P_{out}}{P_{in}} \Rightarrow \eta_{MAX} = \frac{P_{MAX}}{P_{in}}$$

$P_{in}$  is taken as the product of the irradiance of the incident light, measured in  $W/m^2$  or in suns ( $1000 W/m^2$ ), with the surface area of the solar cell [ $m^2$ ]. The maximum efficiency ( $\eta_{MAX}$ ) found from a light test is not only an indication of the performance of the device under test, but, like all of the I-V parameters, can also be affected by ambient conditions such as temperature, intensity and spectrum of the incident light. For this reason, it is recommended to test and compare PV cells using similar lighting and temperature conditions.

**Shunt Resistance ( $R_{SH}$ ) and Series Resistance ( $R_S$ )**

During operation, the efficiency of solar cells is reduced by the dissipation of power across internal resistances. These parasitic resistances can be modeled as a parallel shunt resistance ( $R_{SH}$ ) and series resistance ( $R_S$ ), as depicted in Figure 2.

For an ideal cell,  $R_{SH}$  would be infinite and would not provide an alternate path for current to flow, while  $R_S$  would be zero, resulting in no further voltage drop before the load.

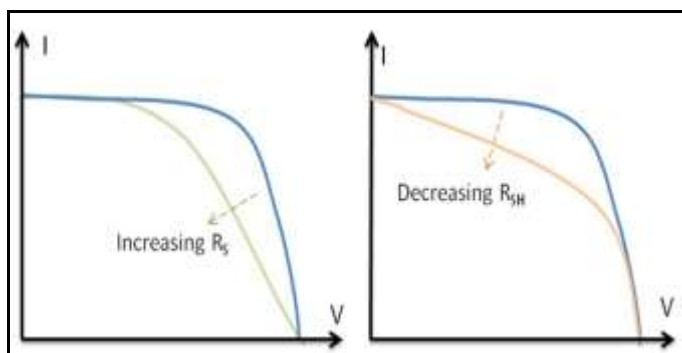


**Figure 6: Effect of Diverging  $R_s$  &  $R_{SH}$  from Ideality**

Decreasing  $R_{SH}$  and increasing  $R_s$  will decrease the fill factor (FF) and  $P_{MAX}$  as shown in Figure 6. If  $R_{SH}$  is decreased too much,  $V_{OC}$  will drop, while increasing  $R_s$  excessively can cause  $I_{SC}$  to drop instead. It is

possible to approximate the series and shunt resistances,  $R_S$  and  $R_{SH}$ , from the slopes of the I-V curve at  $V_{OC}$  and  $I_{SC}$ , respectively. The resistance at  $V_{oc}$ , however, is at best proportional to the series resistance but it is larger than the series resistance.  $R_{SH}$  is represented by the slope at  $I_{SC}$ . Typically, the resistances at  $I_{SC}$  and at  $V_{oc}$  will be measured and noted, as shown in Figure 7.

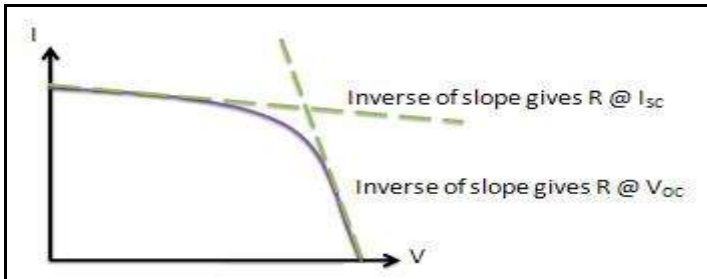


**Figure 7: Obtaining Resistances from I-V Curve**

If incident light is prevented from exciting the solar cell, the I-V curve shown in Figure 8 can be obtained. This I-V curve is simply a reflection of the “No Light” curve from Figure 1 about the  $V$ -axis. The slope of the linear region of the curve in the third quadrant (reverse-bias) is a continuation of the linear region in the first quadrant, which is the same linear region used to calculate  $R_{SH}$  in Figure 7. It follows that  $R_{SH}$  can be derived from the I-V plot obtained with or without providing light excitation, even when power is sourced to the cell. It is important to note, however, that for real cells, these resistances are often a function of the light level, and can differ in value between the light and dark tests.

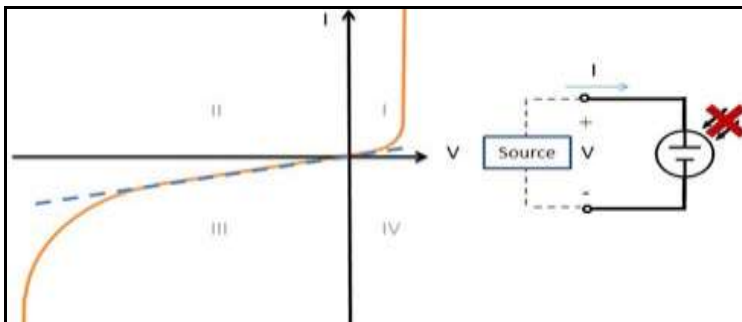


**Figure 8: I-V Curve of Solar Cell Without Light Excitation**

**Temperature Measurement Considerations**

The crystals used to make PV cells, like all semiconductors, are sensitive to temperature. Figure 9 depicts the effect of temperature on an I-V curve. When a PV cell is exposed to higher temperatures, short circuit current  $I_{SC}$  increases slightly, while open circuit voltage  $V_{OC}$  decreases more significantly.

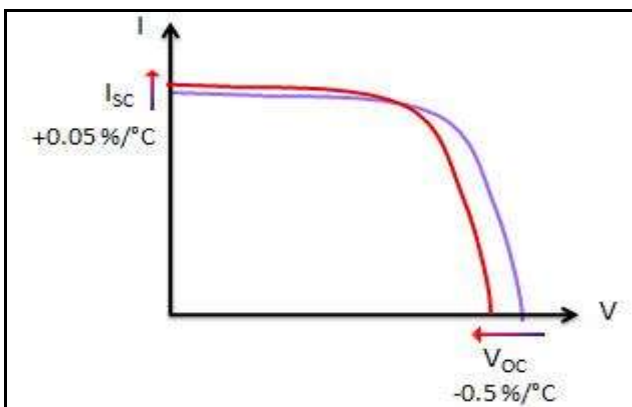


**Figure 9 - Temperature Effect on I-V Curve**

For a specified set of ambient conditions, higher temperatures result in a decrease in the maximum power output  $P_{MAX}$ . Since the I-V curve will vary according to temperature, it is beneficial to record the conditions under which the I-V sweep was conducted. Temperature can be measured using sensors such as RTDs, thermistors or thermocouples.

**III.Block Diagram**

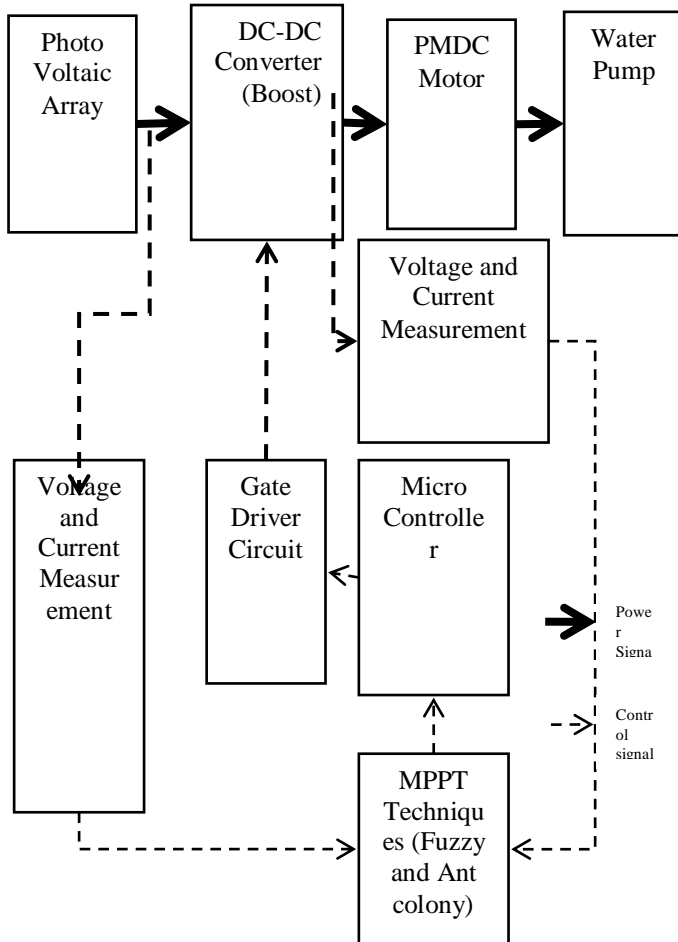


**Figure 10: Generalised block diagram**

**Solar Panel**

A photovoltaic module or photovoltaic panel is a packaged interconnected assembly of photovoltaic cells, also known as solar cells. The photovoltaic module, known more commonly as the solar panel, is then used as a component in a larger photovoltaic system to offer electricity for commercial and residential applications. Solar Panels use light energy (photons) from the sun to generate electricity through photovoltaic effect (this is the photo-electric effect). Most modules use wafer-based crystalline silicon cells or a thin-film cell based on cadmium telluride or silicon. Crystalline silicon, which is commonly used in the wafer form in photovoltaic (PV) modules, is derived from silicon, a commonly used semiconductor. The figure 11 shows the standard solar panel.

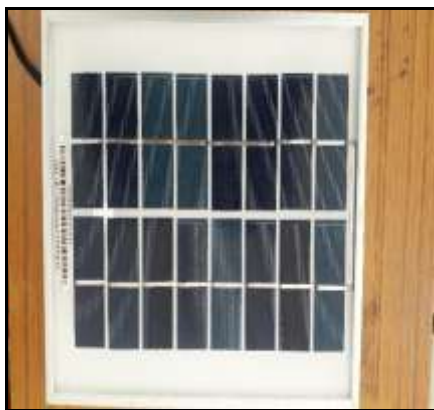


**Figure 11: solar panel**

### **AT89s52 Microcontroller:**

The AT89S52, as shown in figure 12, is a low-power, high-performance CMOS 8-bit microcontroller with 8K bytes of in-system programmable Flash memory. The on-chip Flash allows the program memory to be reprogrammed in-system or by a conventional non volatile memory programmer. By combining a versatile 8-bit CPU with in-system programmable Flash on a monolithic chip, the Atmel AT89S52 is a powerful microcontroller which provides a highly-flexible and cost-effective solution to many embedded control applications. The AT89S52 provides the following standard features: 8K bytes of Flash, 256 bytes of RAM, 32 I/O lines, Watchdog timer, two data pointers, three 16-bit timer/counters, a six-vector two-level interrupt architecture, a full duplex serial port, on-chip oscillator, and clock circuitry. In addition, the AT89S52 is designed with static logic for operation down to zero frequency and supports two software selectable power saving modes. The Idle Mode stops the CPU while allowing the RAM, timer/counters, serial port, and interrupt system to continue functioning. The Power-down mode saves the RAM contents but freezes the oscillator, disabling all other chip functions until the next interrupt or hardware reset.



**Figure 12: AT89s52 Microcontroller**

### **DC-DC Converter:**

An electrical circuit that transfers energy from a DC voltage source to another load is referred to as a DC-DC converter as shown in figure 13. It is a class of power converter, as simple as the name implies, it converts power from one form to another, often as simple as a transformer. DC-DC converters are intended for the decentralized power supply of circuits, assemblies and modules. It is also often required for emergency generators to supply electrical devices from batteries or other DC systems. It is simply a power converter which is used to provide a standard, unregulated, regulated, high isolated or extra wide voltage output for various applications. A dc-dc converter or also known as DC voltage converters can change an input voltage up or

down depending on your needs. It is quite a discerning and worthwhile to learn more about DC-DC converters, why they are necessary, their issues of efficiency and regulation as well. A dc-dc converter is available for step – up and step –down applications and isolated and non –isolated designs.



**Figure 13: DC-DC Converter (Boost)**

### DC Motor

A direct current (DC) motor is a simple electric motor that uses electricity and a magnetic field to produce torque, which turns the motor. At its most, a DC motor requires two magnets of opposite polarity and an electric coil, which acts as an electromagnet. The repellent and attractive electromagnetic forces of the magnets provide the torque that causes the DC motor to turn. The attraction between opposite poles and the repulsion of similar poles can easily be felt, even with relatively weak magnets. A DC motor uses these properties to convert electricity into motion. As the magnets within the DC motor attract and repel one another, the motor turns. The figure 14 shows the DC motor used in this paper.

### Solar Pumping Head

The photovoltaic water pumping systems (PVWPS) is considered as one of the most promising areas in photovoltaic applications. The aim of this work is to determine the effect of pumping head on PVWPS using the optimum PV array configuration, adequate to supply a DC Helical pump with an optimum energy amount.

### IV. Maximum Power Point Tracking

A complete water pumping system is shown in figure 15. A Hybrid MPPT algorithm is proposed to improve the efficiency of photovoltaic (PV) systems under partial shading conditions. Partial shading occurs due to clouds, trees, dirt and dust in PV systems. In partial shading, multiple peaks arise in the PV characteristic curve.



**Figure 14: DC motor**



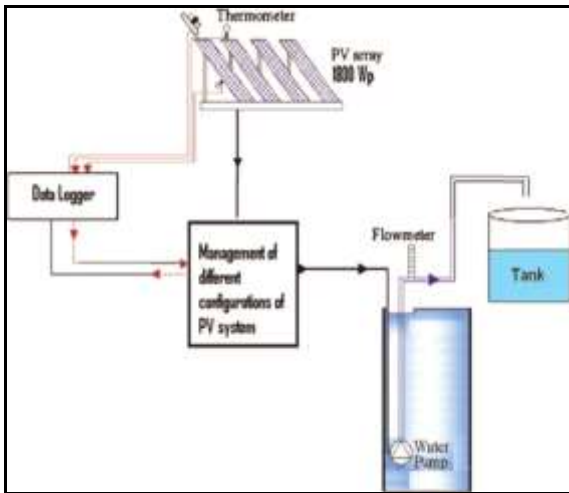


**Figure 15: Control and data acquisition for PV water pumping system**

The maximum power point tracking (MPPT) algorithm adjusts the duty cycle of the switch in DC-DC converter for regulating the input voltage at the Maximum Power Point (MPP) and to provide impedance matching *i.e.* input resistance of converter equal to equivalent solar resistance of PV system at MPP for the maximum power transfer. The Cuk converters have low switching losses and the highest efficiency. Therefore, Cuk converter is chosen as power conditioning circuit to track maximum power using Hybrid MPPT. The influence of algorithm parameters on system behaviour is investigated and the various advantages and drawbacks of the technique are identified for different weather conditions. The variety of available MPPT techniques in literature are summarized by T.Ersam in a form of a survey and he concluded that out of 19 distinct methods found in literature, following three methods are most widely used<sup>2</sup>.

- Perturb and observe(P&O)
- Incremental conductance
- Fractional open circuit voltage

**A.Fuzzy Logic Algorithm**

The Fuzzy Logic Controller block can be divided into four sections: Fuzzification, Rule-Base, Inference and Defuzzification. The FLC inputs turn to fuzzy language in fuzzification section. Then the outputs in inference section are made based on laws of rule-based. In the De fuzzification section, quantifiable results produce from the outputs of inference section. Fuzzy logic is an approach to computing based on "degrees of truth" rather than the usual "true or false" (1 or 0) Boolean logic on which the modern computer is based. In recent years, the number and variety of applications of fuzzy logic have increased significantly. The applications range from consumer products such as cameras, camcorders, washing machines, and microwave ovens to industrial process control, medical instrumentation, decision-support systems, and portfolio selection. The following table gives the rule base for fuzzy logic controller.

**Table 1- The Rule Base For FLC**

$\Delta I$	$\Delta V$	PB	PM	PS	ZZ	NS	NM	NB
P	P	PB	PM	PS	PS	NS	NM	NB
Z	Z	PM	PS		ZZ		NS	
N	N	NB	NM	NS	NS	PS	PM	PB

**Flowchart**

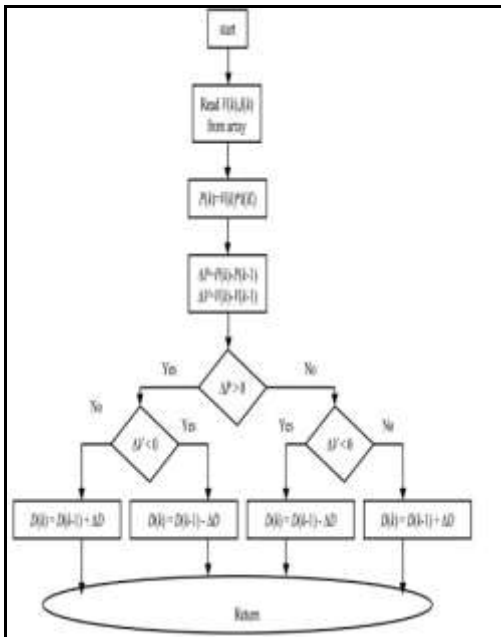


**Figure 16: Flowchart for Fuzzy P&O MPPT tracking algorithm for a Stand-Alone PV system**

**B. Ant Colony Algorithm**

The ant colony optimization algorithm (ACO) is a probabilistic technique for solving computational problems which can be reduced to find good paths through graphs. The first algorithm was aiming to search for an optimal path in a graph, based on the behaviour of ants seeking a path between their colony and a source of food. Ants of some species (initially) wander randomly, and upon finding food return to their colony while laying down pheromone trails. If other ants find such a path, they are likely not to keep travelling at random, but instead to follow the trail, returning and reinforcing it if they eventually find food. The overall result is that when one ant finds a good (i.e., short) path from the colony to a food source, other ants are more likely to follow that path, and positive feedback eventually leads to all the ants following a single path.

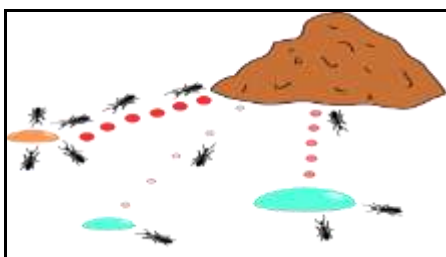


**Figure 17: The ants prefer the smaller drop of honey over the more abundant, but less nutritious, sugar.**

At each stage, the ant chooses to move from one city to another according to some rules:

1. It must visit each city exactly once;
2. A distant city has less chance of being chosen (the visibility);
3. The more intense the pheromone trail laid out on an edge between two cities, the greater the probability that that edge will be chosen;
4. Having completed its journey, the ant deposits more pheromones on all edges it traversed, if the journey is short;
5. After each iteration, trails of pheromones evaporate.

**Flowchart**

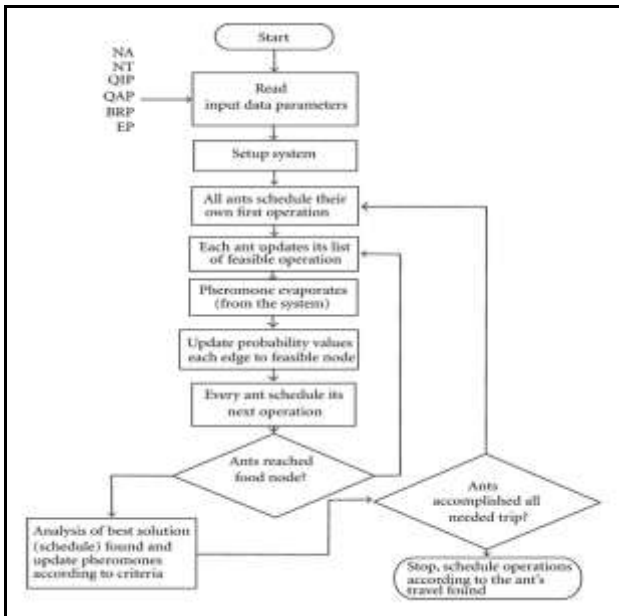


**Figure 18: Flowchart for Ant Colony Algorithm**

**V.Simulation and Results**

The system was tested using MATLAB /SIMULINK model. The system is modelled for single module and then for few module in parallel the figure 19 shows SIMULINK model for PV module with MPPT -Fuzzy logic and Ant Colony.

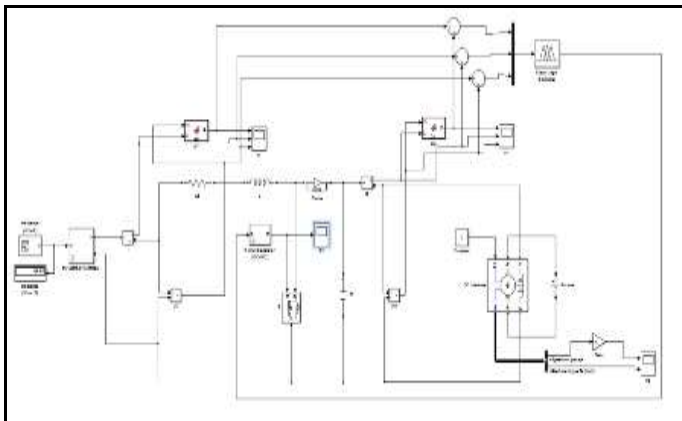


**Figure 19: Simulation Block**

In this MPPT Boost converter is a control block in which MATLAB files are included the voltage, current and power measurement are taken as simulation results. So, the efficiency of solar PV system was improved using Fuzzy logic & ANT-colony algorithm. The battery voltage is controlled using PIC control. The fuzzy rules are shown in figure 20.

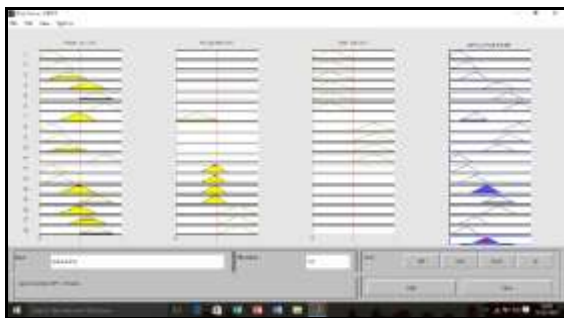


**Figure 20: Rules Using Fuzzy And Ant Colony**

The following figure shows the power, voltage and current waveforms.

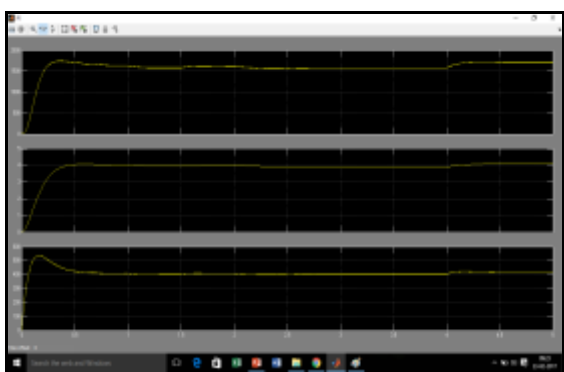


**Figure 21: Power, Voltage And Current Wave Forms**



**Figure 22: Speed-Torque Wave Form of D Motor**

The figure 22 shows the speed –torque waveforms of DC motor.

## VI. Conclusion

In this paper, new technique has been proposed for tracking the maximum power point. The technique is a hybrid of two well-known techniques for MPPT but is equipped with intelligent thinking and therefore has following advantage over the conventional techniques.

- Reach MPP region quickly.
- In case of moving away from MPP as often is the case in *P&O* during environmental variations, this will put us write back in the region of MPP.

## References

1. M. Bahrami, M. Zandi, R. Gavagsaz, B. Nahid-Mobarakeh, S. Pierfederici 'A New Hybrid Method of MPPT for Photovoltaic Systems Based on FLC and Three Point-Weight Methods ', 7th Power Electronics, Drive Systems & Technologies Conference (PEDSTC 2016) 16-18 Feb. 2016
2. Murtaza A., Sher H., Chiaberge M., Boero D., De Giuseppe M., Addoweesh K. (2012). 'A novel hybrid MPPT technique for solar PV applications using perturb & observe and fractional open circuit voltage techniques'. In: 15th International Conference on Mechatronics - Mechatronika 2012, Praga (CZ), December 5-7, 2012
3. P. Nallasivam, C. Jagadeeshwaran. 'A Maximum Power Point Tracking Method Based on Ant Colony Optimization and Particle Swarm Optimization'. International Journal of Revolution in Electrical and Electronic Engineering (IJREEE), 2 Jan 2015.
4. Mohammad R. Al-Soeidat, Alexis Cembrano, Dylan D-C. Lu, SMIEEE University of Technology, Sydney, Australia. 'Comparing Effectiveness of Hybrid MPPT Algorithms under Partial Shading Conditions'. Nsw 2006.
5. A.Terki, A.Moussi, A.Betka, N.Terki Electrical Engineering Department, University of biskra, Algeria. 'An improved Efficiency of Fuzzy Logic Control of PMBLDC for pumping system'. 27 Jan 2011
6. Abou Soufyane Benyoucef, Aissa chouder, Kamal Kara, Santiago Silvestre. 'Artificial bee colony algorithm for maximum power point tracking(MPPT) for pv systems operating under partial shaded conditions' 22 June 2014.
7. S.A.KH. Mozaffari Niapour, S.Dhayali, M.B.B Sharifian, M.R Feyzi, 'Brushless DC motor drives supplied by PV power system based on Z-source and FL-IC MPPT controller. 5 April 2010.
8. M.Benghanem, K.O Daffallah, S.N Alamri, A.A joraid. 'Effect of Pumping Head on Solar Water pump', 19 August 2013.
9. Mohammad Mehdi, seyedmahmoudian, saad mekhilef, Rasoul Rahmani. 'Analytical modelling of partially shaded photovoltaic Systems' 4 Jan 2013.
10. R.ArulMurugan, .Suthanthiravanitha, Department of. ' Model and design of fuzzy-based Hopfield NN tracking controller for standalone PV applications' 3 July 2014
11. Essam E. Aboul Zahab a, Aziza M. Zaki b, Mohamed M. El-sotouhy, 'Design and control of a standalone PV water pumping system', Journal of Electrical Systems and Information Technology, 2017.
12. M. Bahloul, L. Chrifi-Alaoui, M. Souissi, M. Chaabane, S. Drid, ' Effective Fuzzy Logic Control of a Stand-alone Photovoltaic Pumping System', Vol.5, No.3, April 2015.
13. Salas V., Olias E., Barrado A., Lazaro A, ' Review of the Maximum Power Point Tracking Algorithms for Stand-Alone Photovoltaic Systems', Solar Energy Materials & Solar Cells, vol. 90, no.11, pp.1555-1578, 2006
14. Khan, M.T.A. 'Design and performance analysis of water pumping using solar PV', IEEE, Developments in Renewable Energy Technology (ICDRET), 2012 2nd International Conference 2012
15. T. Mhamdi, N. Hidouri, E.Sihem, L. Sbita, E.Sihem A fuzzy controlled-hybrid photovoltaic diesel pumping system, Renewable Energies congress (IREC), 2012
16. Pandikumar Maniraj, Ramaprabha Ramabadran, Ranganath Muthu, 'Analysis of Controllers for Photovoltaic fed Brushless DC Motor based Water Pumping System', Applied Mechanics and Materials, Vol. 787 (2015), pp 838-842, Feb 2015.
17. P.Singhai, S.Gupta, R.Keswani, 'Optimization of PV output for Centrifugal Pumping System Operated by Induction Motor', International Journal of Advanced Scientific and Technical Research, Issue 5 volume 4, pp. 663-673, July-August 2015.
18. Dampuru Naga Sai Saranya, P. V. Subrahmanya Sobhan, 'Fuzzy Logic MPPT Algorithm Assisted PV for PMDC Motor Driven Water Pumping System', International Journal of Scientific Engineering and Technology Research Volume.05, Issue No.18, July-2016, Pages: 3724-3730.
19. Rekioua D, Bensmail S, Bettar N, 'Development of hybrid photovoltaic-fuel cell system for stand-alone application', International Journal Hydrogen Energy. 2014; 39(3):1604–11.

\*\*\*\*\*